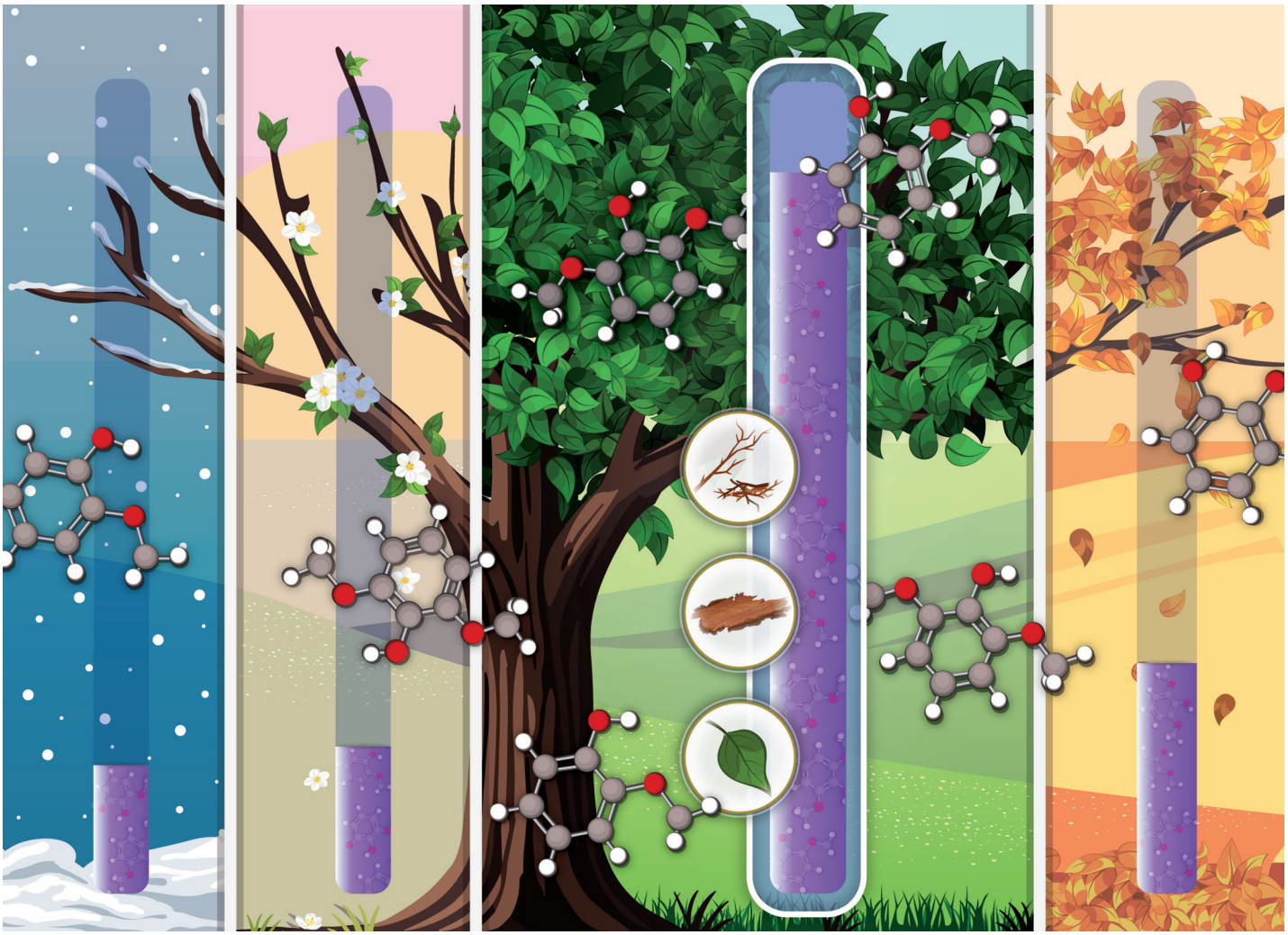

Showcasing research by Robyn C. O'Halloran, Alison J. Shapiro, *et al.* from the groups of Professors Thomas H. Epps, III, Delphis F. Levia, and Dionisios G. Vlachos at the University of Delaware.

Following forest cues for the harvest optimization of tomorrow's biofeedstocks

Forestry residues were harvested from various species and phenophases, characterized, and deconstructed *via* reductive catalytic fractionation (RCF). By targeting the appropriate harvest time, RCF phenolic monomer yields can be tripled. For the first time, a relationship between feedstock selection and lignin valorization was established and used to develop a harvest optimization strategy for forestry residues.

Image reproduced by permission of University of Delaware from *Green Chem.*, 2026, **28**, 827.

As featured in:

See Sunitha Sadula, Dionisios G. Vlachos, Delphis F. Levia, Thomas H. Epps *et al.*, *Green Chem.*, 2026, **28**, 827.

ROYAL SOCIETY OF CHEMISTRY

rsc.li/greenchem

Registered charity number: 207890

Green Chemistry

PAPER

View Article Online
View Journal | View Issue

Cite this: *Green Chem.*, 2026, **28**, 827

Following forest cues for the harvest optimization of tomorrow's biofeedstocks

Robyn C. O'Halloran, †[a] Alison J. Shapiro, †[b] Yagya Gupta,†[b,c] Anna Long,[b] Sara G. Haney,[d] Yuichiro Otsuka,[e] Sunitha Sadula, *[c] Dionisios G. Vlachos, *[b,c] Delphis F. Levia *[a,f,g] and Thomas H. Epps, III *[b,h]

Received 14th August 2025,
Accepted 31st October 2025

DOI: 10.1039/d5gc04279h

rsc.li/greenchem

Renewable feedstocks are a critical component of sustainability and resource security efforts, and feedstock selection is vital for the improved biorefinery production of fuels, chemicals, and materials. A major hurdle for feedstock selection is the inherent heterogeneity and variability among biofeedstocks. Herein, based on knowledge convergence among tree physiological ecology, wood science, and chemical engineering, we present a harvest optimization strategy to maximize lignin valorization in carbon-neutral forestry residues, elucidating the influence of canopy phenophase on possible valorization avenues. This study provides the first report on how tree part, species, and phenophase impact lignin content and deconstruction yields and distributions. Notably, harvesting during the leafed phenophase can double or triple phenolic yields compared to other times of year, offering a simple yet effective strategy to enhance lignin valorization and overall biorefinery production.

Green foundation

1. We demonstrate for the first time that a robust relationship between lignin content and deconstruction products exists as a function of harvest time (specifically phenophase), tree part, and species for forestry residues. Our approach enables strategic feedstock selection and harvest optimization for biorefineries producing more sustainable fuels, chemicals, and materials.
2. Our key achievement is the establishment of a feedstock selection strategy to maximize lignin valorization in forestry residues. Targeting harvest time to the leafed (leafed-spring/summer for pine) phenophase can increase phenolic deconstruction yields up to 3x *vs.* leafless (leafed-winter for pine) or emergence phenophases, and twigs/branchlets from all species and phenophases generate the highest phenolic monomer yields by 2x on a lignin basis.
3. Future efforts can investigate the connection between biofeedstock selection and biorefinery production and environmental impact, to inform harvest optimization that maximizes both product yields and sustainability.

1. Introduction

Fossil fuels currently underpin global energy and chemical production but remain the leading drivers of anthropogenic greenhouse gas emissions worldwide.[1,2] Coupled with escalating resource demands, carbon reduction mandates, and resource security needs, this reliance underscores the desire to transition toward sustainable alternative feedstocks such as lignocellulosic biomass.[3–5] Lignin, the primary source of renewable aromatics, plays a critical role in this transition.[6,7] Yet, the compositional variability and heterogeneity between biofeedstocks remain a critical challenge for their efficient and profitable conversion to valuable products.[8] Thus, understanding lignin's compositional and seasonal variations is fundamental to optimize the generation of high-value bio-derived products. The components of lignin, composed of syringyl (S), guaiacyl (G), and *p*-hydroxyphenyl (H) units,[9] vary significantly depending on the feedstock, environmental con-

[a]*Department of Civil, Construction, and Environmental Engineering, University of Delaware, Newark, DE 19716, USA. E-mail: dlevia@udel.edu*
[b]*Department of Chemical & Biomolecular Engineering, University of Delaware, Newark, DE 19716, USA. E-mail: thepps@udel.edu, vlachos@udel.edu*
[c]*Delaware Energy Institute, University of Delaware, Newark, DE 19716, USA. E-mail: vlachos@udel.edu*
[d]*Department of Chemistry & Biochemistry, University of Delaware, Newark, DE 19716, USA*
[e]*Department of Forest Resource Chemistry, Forestry and Forest Products Research Institute, Tsukuba, Ibaraki 305-8687, Japan*
[f]*Department of Geography & Spatial Sciences, University of Delaware, Newark, DE 19716, USA*
[g]*Department of Plant & Soil Sciences, University of Delaware, Newark, DE 19716, USA*
[h]*Center for Research in Soft matter and Polymers (CRiSP), University of Delaware, Newark, DE 19716, USA*
† The first three listed authors contributed equally to this work, and we make no distinction in first, second, and third author order.

ditions, and phenophases (stages in the annual life cycle of plants).[10–12]

As of 2017, 14% of total global energy was sourced from biomass, with ~85% of that biomass acquired from forests.[13] Of all the biomass sourced from forests, only 8% consists of forest harvesting and manufacturing residues, despite the substantial quantities of these residues generated annually as by-products of logging and milling.[8,13] In the United States, timber harvesting generates nearly 19 million dry tons/y of logging residues, which are typically used in lower-value applications (*e.g.*, heat, power, ash), contributing to environmental degradation and missed economic opportunities.[14] An additional 23 million dry tons/y of logging residues are left in forests (a practice that heightens wildfire risks).[14] With the lignin content of forest residues often exceeding 40 wt% of the total biomass – surpassing that of conventional woody biomass – forest residues represent not just an abundant byproduct but a catalyst for advancing renewable aromatic solutions and reducing dependence on fossil fuels.[15–18] Furthermore, several technoeconomic analysis (TEA) and life cycle assessment (LCA) studies have shown that lignin valorization is key to commercial viability, improving both biorefinery economics and environmental impacts.[19–21] Focusing on higher-value, lignin-derived chemicals, fuels, and materials can transform these underutilized resources into potential drivers of innovation and sustainability in an emerging bioeconomy.

Unlocking the full potential of transforming biomass into high-value products requires fractionation/deconstruction strategies that can efficiently maximize the utility of the entire biomass. One such strategy is reductive catalytic fractionation (RCF), widely regarded as the most prominent lignin-first processing approach for biorefineries.[22–25] RCF mitigates the formation of the lowest-value lignin condensation products and retains the polysaccharide (cellulose, hemicellulose) fraction for subsequent valorization.[25] RCF consistently achieves near-theoretical phenolic monomer yields[26] and produces higher-value components such as monolignols, dimers, and oligomers. These compounds serve as essential precursors for manufacturing lubricants, jet fuels, coatings, monomers/polymers, composites, resins, and biomedical products.[9,27–33] Moreover, S/G/H ratios can directly shape the properties and applications of lignin-derived products.[11,12,34] For example, polymethacrylates composed of S-derived monomers have an ~100 °C higher glass transition temperature than those comprised of G-derived monomers.[35,36] Thus, high S-content polymethacrylates are preferable for producing high-temperature, heat- and flow-resistant materials used in specialty membrane or machine part applications, whereas high G-content polymethacrylates are better suited for thermoformable, boiling-water-stable materials.[35,36] Despite this drastic difference in ultimate properties and application, the influence of phenophase, species, and tree part on lignin content, RCF phenolic monomer yields, and product distribution across tree species and residues remains widely underexplored.

In this study, we optimize informed feedstock selection and harvest scheduling for biorefineries. We reveal how tree parts, species, and phenophase shape lignin content and RCF-based phenolic monomer generation from forest residues. Finally, we discuss how leveraging these insights offers a practical strategy to enhance monomer yields, maximize lignin valorization, and optimize biorefinery performance.

2. Results and discussion

Tree parts (bark, foliage, and twigs/branchlets) of four common co-occurring tree species (American beech, sweet birch, pitch pine, and yellow poplar) common to the eastern United States were collected in each phenophase (senescence, leafless, emergence, and leafed for deciduous species; senescence, leafed-winter (W), emergence and leafed-spring/summer (S) for pitch pine). Note that in this study, the term foliage is used to encompass both the leaves of deciduous species and the needles of coniferous species. Lignin content was measured using the Klason procedure – for discussion of our choice of method, see below.[37] RCF phenolic monomer yields are reported both on a lignin and a biomass basis, and the S/G ratios are those for the RCF monomeric product distributions, which are not necessarily representative of the S/G ratios in the native biomass.

2.1 Lignin characterization method

Lignin quantification for complex feedstocks remains a challenge, and no single 'best' method has yet emerged for the biorefinery field capable of broadly handling all lignocellulosic feedstocks. Short of such a method, the most important consideration for lignin measurements is method consistency, as it enables comparison to lignin measured in other studies, even if a 'true' lignin value is not necessarily obtained.[6] The widespread use of the Klason lignin method in biorefinery literature facilitates comparison between this study and other literature, and measuring all lignin content using the same method throughout this study enables meaningful comparative analysis.[8] We have chosen to use the Klason lignin method herein for consistency and to facilitate comparison, recognizing that the Klason lignin values reported herein may be ~10–20 wt% higher than the 'true' lignin content.[38,39] Additionally, we refrain from combining twigs/branchlets, bark, and foliage data within our analysis in recognition of the likely difference in overestimates between residue types, and we only comment upon the following general trends of lignin contents between residues. For a further discussion of the use of the Klason lignin method for complex feedstocks, see SI section A; for a summary of the lignin characterization methods used in other studies on lignocellulosic residues, see Table S1. 'True' bark lignin quantity is still expected to be higher than woody tissue lignin quantity.[40,41] Bark generally has the highest median lignin content in comparison to twigs/branchlets and foliage across all species and phenophases, aligning with previous reports.[38,41] Median phenolic yields on a lignin basis from twigs/branchlets across species were more than double those from foliage, and bark yields generally fell

between the values for foliage and twigs/branchlets.[15] Limitations of the Klason lignin method for complex feedstocks are further discussed in SI section A.

2.2 Species influence – lignin content

Lignin content is primarily reflective of differing plant functional traits between deciduous and coniferous trees. Lignin content varies across species in all components (p_{bark} < 0.001, $p_{twigs/branchlets}$ < 0.001, $p_{foliage}$ = 0.012, Kruskall–Wallis ANOVA) (Fig. 1). Pitch pine exhibits higher median lignin content in bark and twigs/branchlets relative to deciduous species (Fig. 1). These findings are consistent with previous reports that softwoods typically have higher lignin content than hardwoods.[42] Deciduous trees have more complex xylem tissues, located in the vascular system, and are composed of vessels, tracheids, and wood fibers, whereas pitch pine primarily consists of tracheids.[43] The higher lignin content in pitch pine twigs/branchlets may stem from the prevalence of tracheids, which have thicker, more lignified walls than deciduous trees' vessels and fibers. Phloem tissue, adjacent to the xylem, is present in the twigs/branchlets of all species and also contributes lignified cells like sclereids and fibers to the overall lignin content. Given that twigs/branchlets have smaller interquartile and overall ranges than bark and foliage, phloem compositions may be less variable than xylem compositions.[43] Among deciduous species, sweet birch exhibits the highest median lignin content for bark and twigs/branchlets. Yellow poplar bark lignin content exceeds that of American beech bark but is lower for twig/branchlets content (Fig. 1). Lignin content data are shown in Tables S2 and S3.

2.3 Species influence – total phenolic yields and S/G ratios

The differences in RCF product distribution between species also can be attributed to the anatomical structure of coniferous and deciduous trees. Both total phenolic yield and S/G ratio for each residue, species, and phenophase are shown in Fig. 2. It is well established that softwoods are composed almost exclusively of G units, whereas hardwoods have a mix of S and G units.[25,44,45] Unsurprisingly, pitch pine residues are

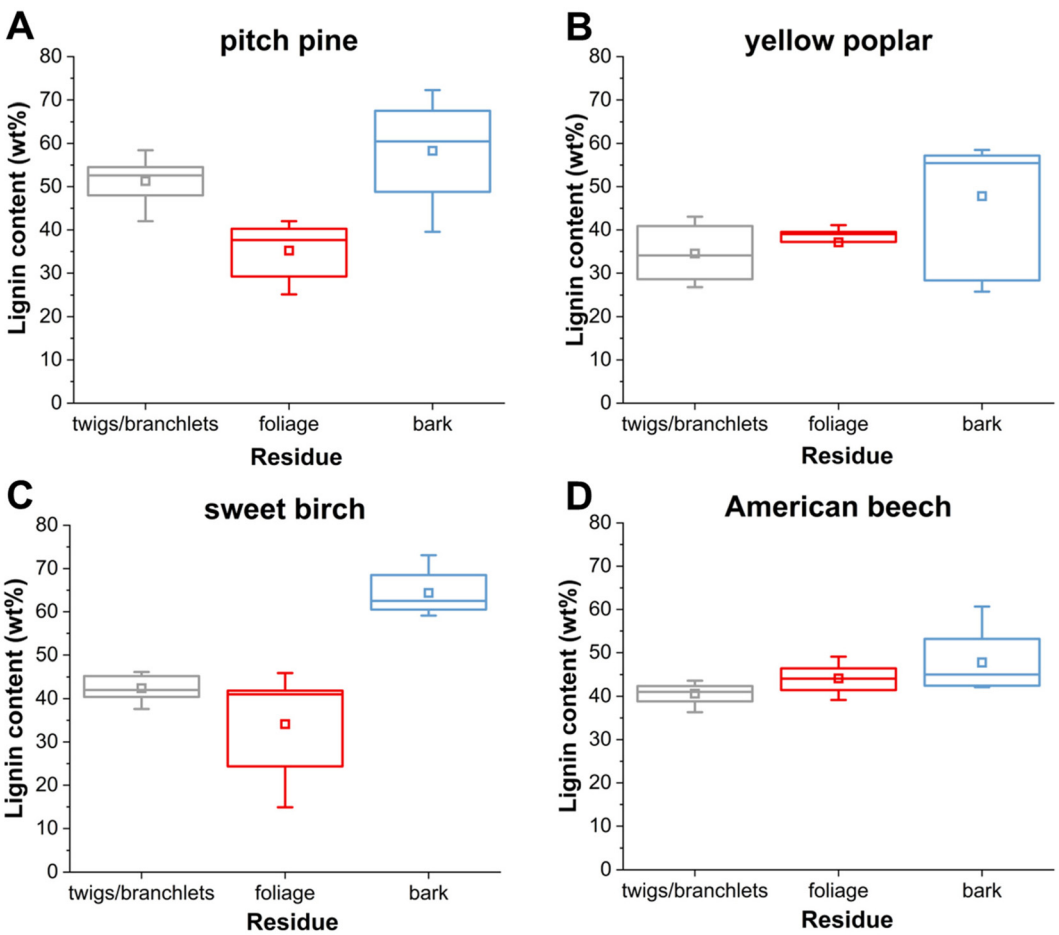

Fig. 1 Box plots of lignin content (wt%) (on a dry, extractive-free basis) for (A) pitch pine, (B) yellow poplar, (C) sweet birch, and (D) American beech forest residues for all phenophases. Twigs/branchlets are shown in gray, foliage in red, and bark in blue. Note that the leafless phenophase of deciduous species overlaps with the leafed (W) phenophase of pitch pine. The box indicates the interquartile range of the data spanning from the first to the third quartile. The whiskers indicate the minimum and maximum data points, the square within the box denotes the mean, and the horizontal line inside represents the median (50th percentile).

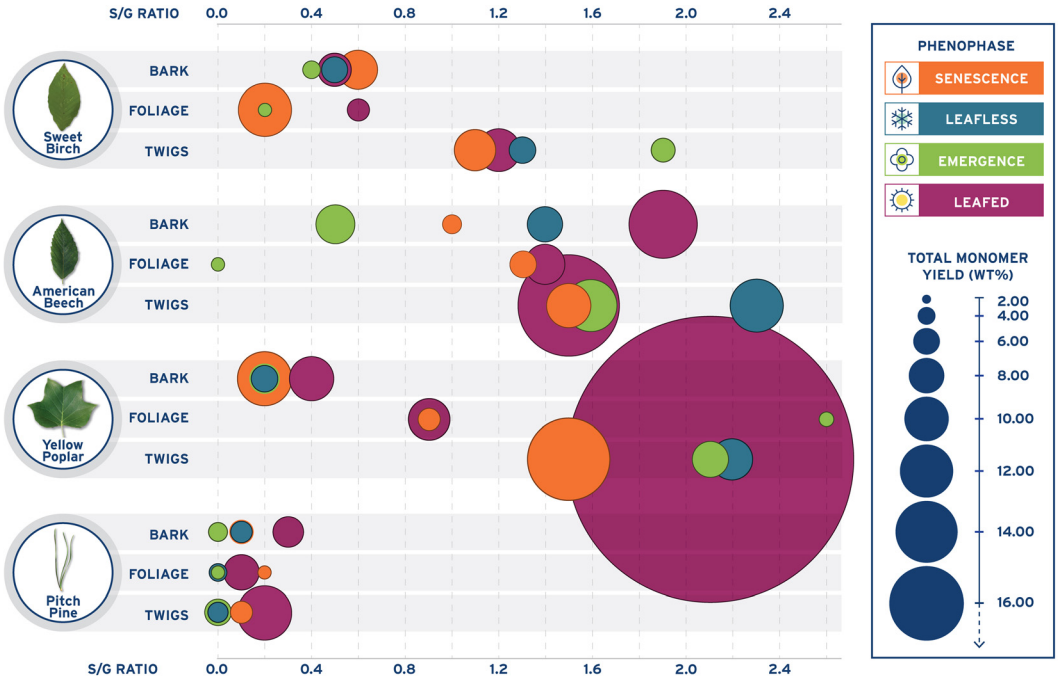

Fig. 2 Total phenolic monomer yields (wt%) (on a dry, extractive-free lignin basis) and S/G ratio of twigs/branchlets, foliage, and bark for all species across all phenophases. Senescence is shown in orange, leafless/leafed (W) in blue, emergence in green, and leafed/leafed (S) in magenta. The circle's center aligns with the row's center, indicating the residue type. Circle size indicates monomer yield, with increased size indicating increased yields. The *x*-axis indicates the S/G ratio for each species and residue type. Reported as mean with $n = 3$.

dominated by G units and therefore have a significantly lower S/G ratio than deciduous species ($p < 0.001$, Kruskall Wallis ANOVA) (Fig. 2). Among deciduous species, twigs/branchlets generally exhibit the highest S/G, and American beech has the highest S/G ratio for bark and foliage (Fig. 2). Sweet birch has a higher S/G ratio in bark compared to that of yellow poplar yet a lower ratio in foliage (Fig. 2). Phenolic monomer yields show significant variation among species for twigs/branchlets, bark, and foliage ($p = 0.009$), with pitch pine residues having significantly lower yields than American beech ($p = 0.011$). This finding aligns with previous studies that have reported that softwoods tend to have lower monomer yields than hardwoods, which has generally been attributed to increased C–C linkages associated with more G units.[10,46] There is a relatively strong correlation (Pearson correlation coefficient = 0.87, Table S6) between the total monomer yield and S unit yield; however, as was demonstrated by Anderson *et al.*, the S/G ratio alone cannot predict RCF yields as additional factors, important to lignin biosynthesis, affect the ultimate ratio of C–O/C–C bonds in plants during lignification, such as lignin monomer concentrations and delivery rates of monomers to the cell wall.[47] Furthermore, monomer yields and S/G ratios are also impacted by RCF parameters, such as the choice of catalyst.[11] It is worth noting that although S, G, and H units are the primary monomeric units in lignin, they are by no means the only phenolic structures that may be present, especially when considering terminal or grated units.[48,49] Additional lignin monomeric units that may be incorporated in lignin include *p*-hydroxybenzoates and ferulates as well as their derivates, although lignin biosynthesis remains an active field of work.[48,49] RCF monomer yield and distribution data and monomer yield box plots are shown in Tables S4, S5 and Fig. S1, respectively.

2.4 Phenophase influence – lignin content

Lignin content varies across phenophases in bark and foliage, whereas twigs/branchlets maintain a consistent lignin quantity throughout the year ($p_{bark} = 0.002$, $p_{twigs/branchlets} = 0.218$, $p_{foliage} = 0.020$, Kruskal–Wallis ANOVA) (Fig. 3). Bark lignin content shows the largest variability during the change of seasons from leafed/leafed (S) to leafless/leafed (W) (or *vice versa*), with the lowest amount during senescence and highest in emergence (Fig. 3). Foliage exhibits the lowest lignin content in senescence, with content increasing progressively through emergence to the leafed/leafed (S) phase (Fig. 3). Notably, pitch pine, the sole species with foliage in the leafless/leafed (W) phase, displays a foliage lignin content similar to the overall median foliage lignin content across all species and phenophases (Fig. 3).

Phenophase-specific changes, particularly in bark and foliage, reflect adaptive shifts in lignin content and biosynthesis that influence feedstock properties throughout the growing season. The limited variability of lignin content in twigs/branchlets across phenophase indicates less susceptibility to phenological changes. In contrast, bark lignin content varies across phenophase, potentially reflecting shifts in physiological priorities. The relatively low lignin content in bark during senescence may reflect a shift in physiological priori-

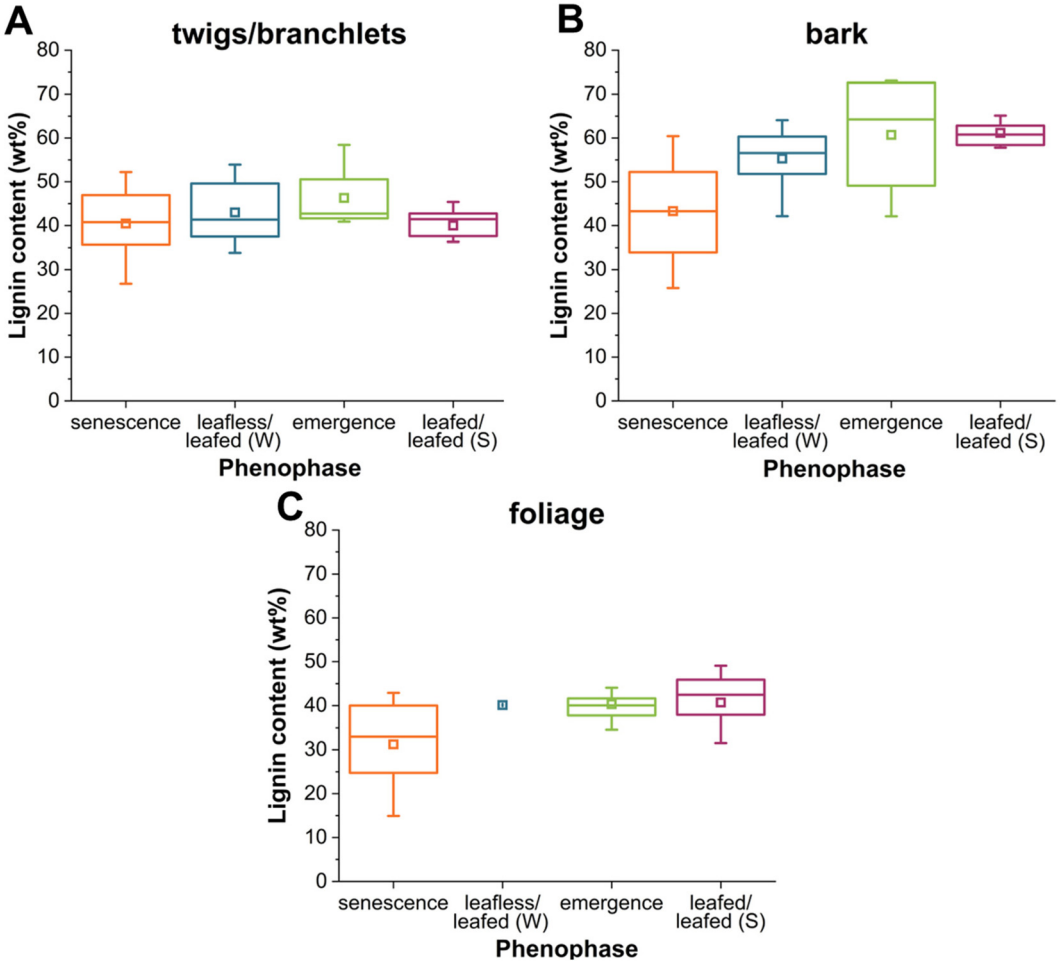

Fig. 3 Box plots of lignin content (wt%) (on a dry, extractive-free basis) in (A) twigs/branchlets, (B) bark, and (C) foliage of different species across phenophases. Senescence is shown in orange, leafless/leafed (W) in blue, emergence in green, and leafed/leafed (S) in magenta. The box indicates the interquartile range of the data spanning from the first to the third quartile. The whiskers indicate the minimum and maximum data points, the square within the box denotes the mean, and the horizontal line inside represents the median (50th percentile). Note that deciduous species do not have foliage in the leafless phenophase – therefore, only the pitch pine is represented in the mean for this phenophase.

ties from growth to defense and nutrient conservation, consistent with patterns of nutrient resorption observed during leaf senescence.[50] Higher bark lignin content during the leafless/leafed (W) phase than senescence may suggest increased lignin deposition for added structural support and protection in the absence of foliage. The similarly high bark lignin contents in leafed/leafed (S) and emergence phases suggest that a common underlying mechanism drives lignin deposition during these phases despite their distinct physiological contexts. Interestingly, sweet birch bark has the highest lignin content, which possibly enhances resistance to decay and insect damage, thereby conferring a selective advantage in its native habitats.[51] A similar trend in lignin content was noted in foliage across phenophase. The apparent reduction in lignin during senescence may be due to the degradation and recovery of inorganic salts, chlorophyll, and other factors that the Klason method may overestimate;[6] however, the lignification process occurs gradually as foliage matures, explaining the intermediate lignin levels of emerging relative to fully developed foliage during the leafed/leafed (S) season.

2.5 Phenophase influence – total phenolic yields and S/G ratios

All tree parts produce the highest total phenolic monomer yields during the leafed/leafed (S) phenophase (Fig. 2 and S2). Total phenolic monomer yields are comparable in senescence, leafless, and emergence phenophases for bark (Fig. 2). Twigs/branchlets and foliage show a significant phenological variation ($p_{\text{twigs/branchlets}} = 0.040$, $p_{\text{foliage}} = 0.009$, Kruskal Wallis ANOVA), and the leafed/leafed (S) phase exhibited the largest phenolic monomer yields by senescence emergence (Fig. 2). In the leafless/leafed (W) phase, pitch pine foliage yields are between those of senescence and emergence, whereas twigs/branchlets yields are at their lowest during this phenophase (Fig. 2). Higher total phenolic monomer yields during the leafed/leafed (S) phase compared to emergence may indicate a greater abundance of β-O-4 bonds during the leafed/leafed (S)

stages and that lignin condensation may be impacted by phenophase, although future studies are needed to quantify the relative fraction of β-O-4 bonds across seasons and confirm this hypothesis.

The S/G ratio is relatively constant across phenophases (p = 0.836, Kruskall Wallis ANOVA); notably, this relative lack of phenological change is due to the G and S unit yields following similar phenological patterns rather than remaining stable throughout the year. For instance, G unit yields are significantly influenced by the time of year ($p_{g\ units}$ = 0.001, Kruskal Wallis ANOVA) and are highest during the leafed/leafed (S) phase, followed by senescence, leafless/leafed (W), and emergence. S units follow the same variation pattern as G units by phenophase, although not statistically significant ($p_{s\ units}$ = 0.062, Kruskall Wallis ANOVA), peaking in the leafed/leafed (S) phase, followed by senescence, leafless/leafed (W), and emergence (Fig. 2).

2.6 Combined influence of tree part, species, and phenophase on phenolic monomer yields

Total monomer yields per unit biomass (Fig. 4 and Table S5) highlight the significant impact of phenophase on monomer production, with foliage yielding the lowest and bark and twigs showing more comparable results. Box plots of total phenolic monomer yield grouped by species and phenophase are shown in Figs. S3 and S4, respectively. These yields account for both the total lignin content and the RCF monomer yield, providing a value for the total yield from biomass measured prior to fractionation. Total monomer yields per unit biomass generally are the lowest for foliage and comparable between bark and twigs (*e.g.*, emergence yellow poplar yields are 3.8 ± 0.3, 3.5 ± 0.5, and 1.3 ± 0.2 wt% for bark, twigs/branchlets, and foliage, respectively; Fig. 4). Consistent with the trends noted above on a lignin basis, phenophase has a much greater impact on the yield than species. Most notably, the leafed/leafed (S) phenophase has the greatest total monomer yields, often by several wt% in all but two instances. The five highest total monomer yields are all in the leafed/leafed (S) phenophase: American beech bark, yellow poplar twigs/branchlets, American beech twigs/branchlets, yellow poplar bark, and pitch pine twigs/branchlets (Fig. 4). The two exceptions are sweet birch twigs/branchlets, in which the senescence and leafed phenophases equivalently have the highest yields, and sweet birch bark, in which the leafed phenophase has the second highest yield behind senescence (Fig. 4 and Table S5).

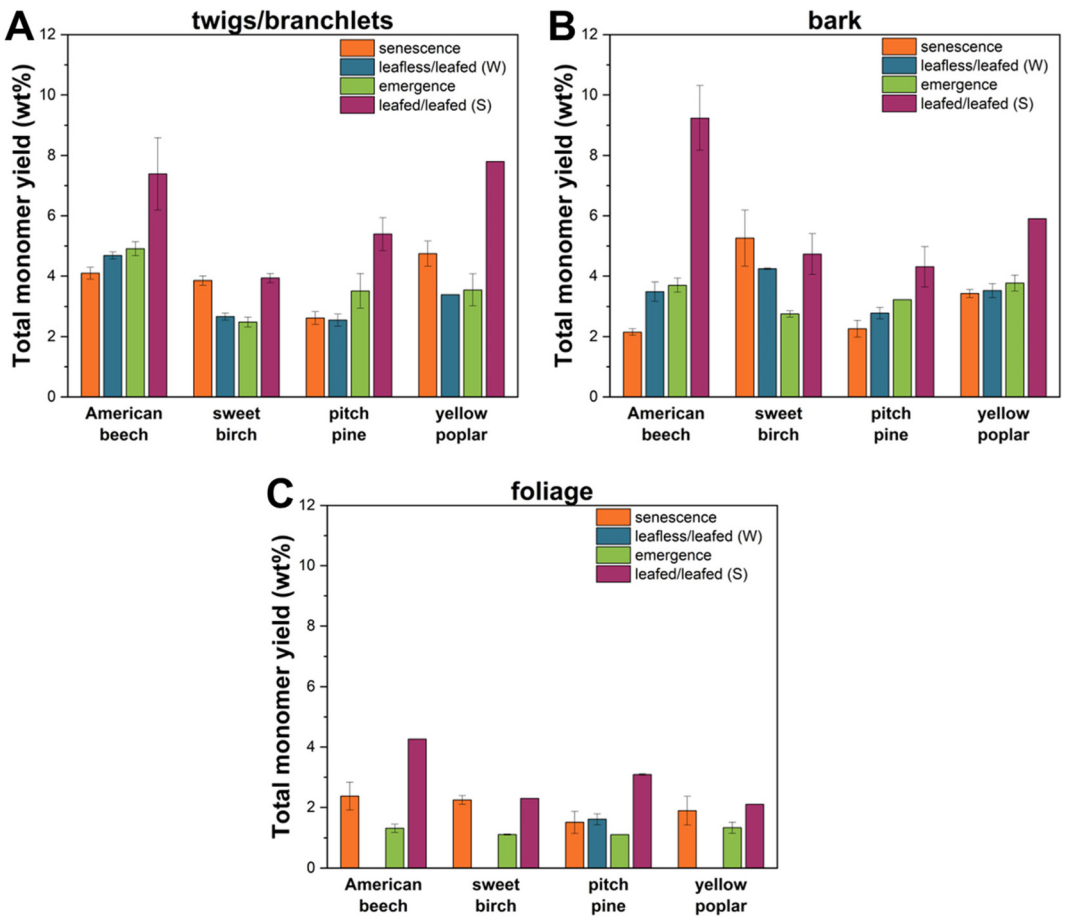

Fig. 4 Total phenolic monomer yields (wt%) on a dry, extractive-free biomass basis for (A) twigs/branchlets, (B) bark, and (C) foliage. Senescence is shown in orange, leafless/leafed (W) in blue, emergence in green, and leafed/leafed (S) in magenta. Note that for deciduous species, there is no foliage in the leafless phenophase. Reported as mean ± standard deviation.

The phenophase with the lowest total monomer yield is most often emergence or senescence. While twigs/branchlets do not follow a specific trend by phenophase, foliage consistently has its lowest phenolic monomer yield during emergence. Bark generally shows the lowest phenolic monomer yields during senescence, except for sweet birch bark, which has its highest yield in senescence. Interestingly, sweet birch is the only species for all residues with the lowest monomer production consistently occurring in a single phenophase – emergence.

2.7 Harvest optimization for biorefineries

Forest residues are attractive biorefinery feedstocks due to their relatively low cost and abundance. They are already collected as byproducts from logging and sawmills but are generally used for lower-value applications such as energy generation or compost.[8] Forest residues often have higher lignin contents than woody biomass.[8,13,15,16] Higher lignin contents may reduce the value of the compost because lignin is particularly challenging to degrade under typical composting conditions, ultimately making forest residues better suited to other applications.[52] The total phenolic monomer yields from forest residues generally are lower (<10 wt% on a biomass basis; <30 wt% on a lignin basis) compared to wood (typically 20–60 wt% on a lignin basis for native woods),[42] which reflects structural constraints in these residues. For instance, reduced yields in bark may be attributed to the presence of suberin and a more condensed lignin structure with fewer C–O bonds, as noted in black locust bark.[39] To quantify the impacts of the lower yields of residues compared to woody feedstocks on the biorefinery economics and sustainability, TEAs and LCAs are useful (similar to recent work performed on a yellow poplar residue-based biorefinery).[15] It is important to note that the economic viability of biorefinery will also depend on factors such as the market for renewable phenolics and biorefinery scalability.[15,19] Furthermore, although analyses in this study were performed on an extractive-free, dry basis, both moisture and extractive content can be important factors for a biorefinery. Residues often have higher moisture/extractive content than traditional woody biomass, which should be considered, as drying can be energy-intensive and significantly contributes to overall biorefinery greenhouse gas emissions.[53] Another practical consideration is that biomass collection may depend on access to logging sites, and its availability/cost may be influenced by external factors like forest health and weather events.[8,54] Additionally, the total biomass available during each phenophase is inherently site- and stand-specific, depending on species composition, forest structure, and local climate.[55] Thus, to translate phenophase-specific monomer yields into total monomer production, biorefineries should integrate local forest inventory data and seasonal biomass dynamics into their analyses for TEA/LCA projections. Overall, TEA and LCA are critical next steps to connect these harvest optimization strategies proposed herein directly to their economic and environmental impacts for industrial biorefineries.

Forest residues may also be collected together, with different tree parts mixed in a single RCF reaction. A limited number of experiments were performed to determine the agreement between predicted cumulative yields when tree parts are combined at a known ratio (Fig. S5). Good agreement (within error) was found between predicted and experimental cumulative yields when tree parts were mixed at known ratios for sweet birch, and reasonable agreement (within 2 wt%) was seen for pitch pine. This agreement may suggest that tree part combination does not interfere with the RCF reaction progression for sweet birch and pitch pine; however, quantitative conclusions are limited due to the small sample size. Biorefineries and RCF experiments involving tree part combinations should conduct more extensive studies to verify these results and potentially optimize RCF conditions to enhance phenolic yields further. For instance, recent work has demonstrated that certain RCF conditions enable efficient deconstruction of a wide range of lignocellulosic biomass feedstocks in a scalable feedstock-agnostic process.[56] The efficiency and selectivity of RCF are strongly influenced by both catalyst characteristics (*e.g.*, type, dispersion, support) and reaction conditions.[57–61] Metal choice (*e.g.*, Ru, Ni, Pt, Pd) and the use of external hydrogen or hydrogen-transfer reagents can significantly affect monomer yields and product distributions. Hydrogen-free RCF is a promising method, and the choice of solvent and catalyst pair is key to control product selectivity of aromatic monomers.[59] Thus, optimizing RCF conditions and combinations is essential to maximize monomer yields and control product distributions in biorefinery applications.

An overview of the harvest optimization strategies established herein is shown in Fig. 5. Biorefineries should prioritize using barks and twigs/branchlets from all phenophase and species over foliage to maximize total phenolic yields, as bark consistently exhibits high lignin content, and twigs/branchlets consistently produce double the amount of total phenolic monomers than bark. Biorefineries can more than double total monomer yield and maximize lignin valorization by harvesting forest residues during the leafed/leafed (S) phenophase. American beech and yellow poplar bark and twigs/branchlets and pitch pine twigs/branchlets in the leafed/leafed (S) phenophase achieve the highest total monomer yields on a biomass basis, thus serving as the optimal biorefinery feedstocks. In contrast, sweet birch does not reach the same peak yields, but its consistency across phenophases may benefit biorefineries with less inventory management capacity, seeking consistent yields throughout the year.

S/G ratio variation can significantly impact the properties of polymers synthesized from phenolic monomeric units, thus determining the ultimate application of lignin-derived materials (due to structure–property relationships discussed in the introduction).[34–36] Understanding the relationship between feedstock selection and S/G ratios enables biorefineries to manage inventory and predict/tailor biorefinery outputs. To target low S/G ratios, softwood residues can be harvested in any phenophase. Conversely, to target high S/G ratios, biorefineries should use deciduous twigs/branchlets (especially those of American beech and yellow poplar) in any phenophase. To maximize both G and S unit yields, harvests

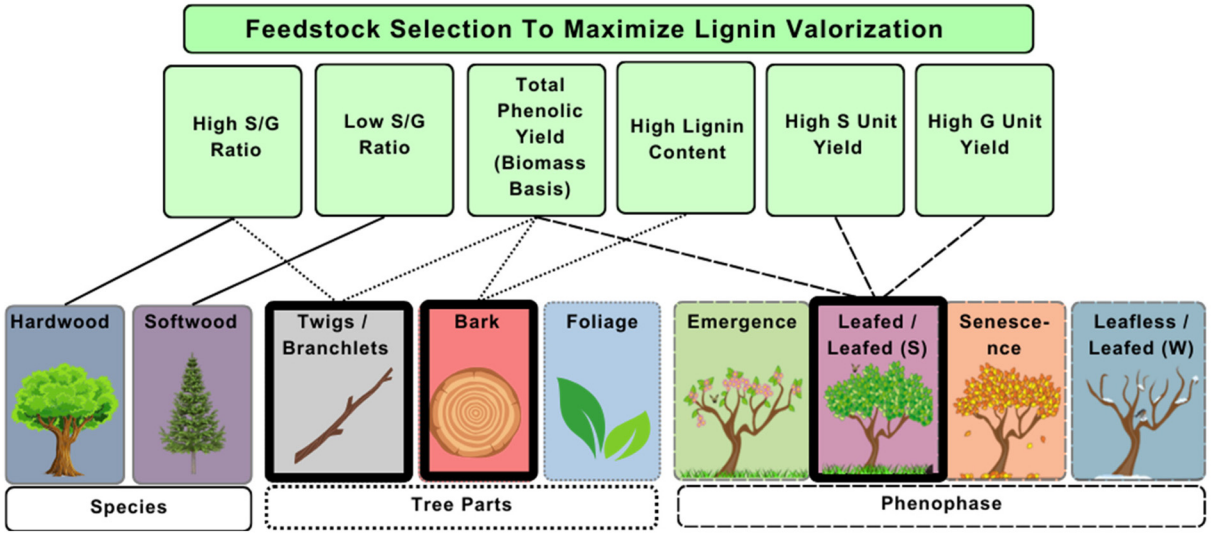

Fig. 5 Overview of forest residue harvest optimization strategies to maximize lignin valorization in lignocellulosic biorefineries. Lines to optimal species, tree parts, and phenophases are shown with solid, dotted, and dashed lines, respectively. Species are grouped into two broader categories: hardwoods (American beech, sweet birch, and yellow poplar) and softwoods (pitch pine). Twigs/branchlets, bark, and leafed/leafed (S) are highlighted with a bold black outline as the recommended feedstocks for biorefineries to maximize lignin valorization.

should be conducted during the leafed/leafed (S) phase. The correlation between higher S unit yields and total phenolic yields across all tree parts, species, and phenophases indicates that biorefineries should target higher S unit-containing residues; however, this point must be made with a few caveats. First, the S unit values reported herein are as quantified after RCF, which has been a popular method for lignin structure analysis for nearly a century and may be representative of the ratios in the native lignin but has not been fully established as an analytical approach to determine S/G ratios.[6] Second, typically G units are more condensed than S units due to the availability of the C5 position on the aromatic ring in G units that is available for radical coupling.[62] Thus, S units are typically more involved in β-ether bonds (*e.g.*, β-O-4 bonds) but also β–β bonds (a condensed C–C bond).[62] Third, higher S units may be associated with higher monomer yields, but lignin bond speciation is impacted by additional factors during biosynthesis (*e.g.*, monomer concentrations and delivery rates), which remains an active area of biorefinery research.[6,47]

A final consideration for the harvest optimization of forestry residues is the biogeographic ranges of the species examined. The tree species studied here grow primarily within the Eastern temperate deciduous forest biome. As such, the phenophase-driven differences in lignin content and monomer yields observed here may vary in magnitude or timing from other biomes with different climatic or edaphic conditions, species assemblages, or management systems. Moreover, although the results herein provide insight into general patterns of seasonal lignification in temperate Eastern U.S. forests, additional studies across broader geographic and climatic gradients are needed to evaluate the robustness and global applicability of these findings.

3. Conclusions

Strategic feedstock selection and harvest optimization offer significant potential to address critical challenges, including resource scarcity, supply chain inefficiencies, and the underutilization of biomass resources. These conclusions are drawn from trees native to Eastern U.S. forests, yet the principles of optimizing harvests can be applied globally, extending to other forest ecosystems, agricultural residues, and municipal waste streams, all of which exhibit spatial and temporal variances. By leveraging these strategies, we can enhance not only the value of forest residues but also reduce environmental impacts, mitigate waste, and drive sustainability across multiple sectors. Lignin valorization is essential to the commercial success of biorefineries, improving economics and mitigating environmental impacts. Furthermore, as global demand for renewable fuels, chemicals, and materials continues to rise, these approaches are vital to scaling up the bioeconomy, ensuring energy security, and reducing dependency on fossil fuels. Ultimately, these innovations could catalyze a fundamental shift towards a more circular economy in which bioresources are utilized to their fullest potential, and the integration of these strategies within industrial biorefineries leads to a more sustainable, resource-efficient, and resilient future.

4. Experimental section

4.1 Study site and field collection

Biomass samples (foliage, bark, twigs/branchlets) from the four test species – *Betula lenta* L. (sweet birch), *Fagus grandifolia* Ehrh. (American beech), *Liriodendron tulipifera* L. (yellow poplar), and *Pinus rigida* Mill. (pitch pine) – were collected

during each phenophase (senescence, leafless, emergence, and leafed for deciduous species; senescence, leafed (W), emergence, and leafed-spring/summer (S) for pitch pine) from the mixed species forest within and near the Fair Hill Natural Resources Management Area (39°42′ N, 75°50′ W) in northeastern Maryland. For each phenophase, biomass samples were collected from multiple individuals of each species of varying size, height, and age, ensuring that samples were representative of each tree species examined. Bark samples consisted primarily of outer bark, especially from the thicker, rough-barked species (*e.g.*, yellow poplar, pitch pine). The depth of outer bark inherently varies with species-specific bark thickness and tree age. The tree species examined represent a range of traits. For example, American beech is shade tolerant, whereas yellow poplar is shade intolerant. Pitch pine is the only gymnosperm, whereas the other three tree species are angiosperms. Such differences are noteworthy because differing traits among species lead to differing life strategies that impact the biomass structure and chemical composition.

4.2 Materials

The collected biomass samples were dried in an oven at 40 °C to <10 wt% moisture (approximately 12 to 48 h).[37] Moisture content was determined *via* a Sartorius moisture content analyzer (MA 160). Dried biomass was milled to a <0.5 mm powder size using a Thomas Wiley® Mini Cutting Mill. Methanol (certified ACS Reagent Grade, 99.8%), hexanes (98.5%), and sulfuric acid (certified ACS plus, 95.0–98.0%) were purchased from Fisher Scientific. 5 wt% Ru/C powder (MKCQ0667) and decane (99.8%) were purchased from Sigma Aldrich. Ethanol (200 proof, anhydrous) and sulfuric acid (72% w/w) were purchased from Decon Laboratories and Ricca Chemical, respectively. All chemicals were used as received.

4.3 Lignin compositional analysis

After collection, drying, and milling of the biomass, extractives were removed according to previously reported procedures to reduce lignin measurement interference.[6] Briefly, samples were sonicated in 80 vol% ethanol in deionized water at least four times, followed by sonication in hexanes at least two times until the solvent wash ran clear. Samples were subsequently dried under a dynamic vacuum at 40 °C for at least 48 h. Moisture and extractive content data are shown in Table S7. Biomass compositions were measured using a procedure from the National Renewable Energy Laboratory.[37] In this procedure, dried, extractive-free biomass underwent a two-step acid hydrolysis following the Klason procedure for lignin analysis. The lignin was fractionated into acid-soluble and insoluble material, measured by Ultraviolet–Visible spectroscopy (240 nm) and gravimetric analysis, respectively. The Klason method is known to overestimate lignin content in non-woody biomass, such as foliage and bark, due to non-woody tissues containing more complex residues (*e.g.*, tannins, inorganic salts, proteins, fats, waxes) that are not degraded or solubilized in the two-step acid hydrolysis,[6] as discussed further in SI section A.

4.4 RCF

RCF was performed as described in the literature.[9,15] Briefly, 0.1 g Ru/C and 1 g of biomass were added to 20 mL of methanol in a 50-mL, high-pressure, Parr reactor. A heating jacket, connected to a variable power supply and controlled by a proportional-integral-derivative temperature controller, was used to heat the reactor to 250 °C. The RCF conditions were established in previous work.[9] Reaction temperature was monitored using a K-type thermocouple in a thermowell. The reactor was purged three times with N_2, pressurized with 40 bar of H_2, and stirred for 15 h at 250 °C. The stir rate was 500 rpm, and reactions were performed in duplicate. Subsequently, the reactor was passively cooled to 25 °C, and the H_2 was released. Reaction products were filtered using 0.45-μm Nylon syringe filters to aid in phenolic monomer identification and quantification.

4.5 RCF product identification and quantification

RCF products were identified *via* gas chromatography-mass spectrometry (GC-MS) and quantified *via* GC-flame ionization detector (GC-FID) analysis. An Agilent 7890B series GC instrument, fitted with an HP5-MS capillary column, and an Agilent 5977A series MS instrument, were employed for the GC-MS analysis of the reaction products at the following conditions: injection temperature of 250 °C, column temperature program of 50 °C (1 min), ramp to 300 °C at 15 °C min^{-1}, hold at 300 °C (7 min). The transfer line connecting the GC instrument to the MS instrument was maintained at a detection temperature of 290 °C to ensure efficient transfer of the analytes. Both the FID and MS used helium as the carrier gas at a flow rate of 25 mL min^{-1}.

The phenolic monomers in the reaction product were quantified using an Agilent 7890B series GC instrument, equipped with an HP5 column and an FID. The injection and detection temperature were 300 °C. The column temperature program included a 40 °C hold (3 min), a ramp to 100 °C at 30 °C min^{-1}, a ramp to 300 °C at 40 °C min^{-1}, and a hold at 300 °C (5 min). GC-FID chromatogram peaks are arranged in the same order as those in the GC-MS chromatogram because a similar capillary column was used. The effective carbon number (ECN) method and an internal standard (decane) were used to quantify phenolic monomers as standard monomers were not available. Based on lignin mass content, phenolic monomer yield was determined by calculating integrated areas of the monomer and decane in the GC chromatograms, as described in the literature.[9,63] Twelve phenolic compounds were identified, including typical guaiacyl and syringyl derivatives. For the full list of compounds, see SI section B.

4.6 Statistical analysis

Median values for overall trends and mean values and standard deviations of individual tree part, species, and phenophase are shown in Tables S2/S3 and S4/S5, respectively. Extractive and moisture content are shown in Table S7. Yellow poplar leafed phenophase data was obtained from a previously published paper.[15] Statistical differences (p-value <0.05) were deduced using two-way ANOVA. Assumptions of normality and

homogeneity of variances were verified *via* the Shapiro–Wilk and Brown–Forsythe tests, respectively. An appropriate two-way ANOVA (such as the Kruskal Wallis test for non-normal data) was then performed on the basis of these assumptions. If significant results were obtained, Dunn's test for multiple pairwise comparisons was employed to pinpoint statistically significant differences. The ANOVA revealed non-significant *p*-values for small sample sizes ($n = 3$), introducing larger deviations. For such cases, we considered mean differences within 2 wt% as not statistically different, indicating practical equivalence despite potential fluctuations.[15] This approach enabled us to identify meaningful trends from the data, acknowledging the statistical limitations. All statistical analyses were conducted using SigmaPlot v. 15.0.

Conflicts of interest

There are no conflicts to declare.

Data availability

All data supporting the findings of this study are available within the article and its supplementary information (SI) or from the authors upon reasonable request.

Supplementary information is available. See DOI: https://doi.org/10.1039/d5gc04279h.

Acknowledgements

This work was supported by the National Science Foundation Growing Convergence Research program (NSF GCR CMMI 1934887) in Materials Life-Cycle Management. The authors express their gratitude to the Fair Hill Natural Resources Management Area for permission to access their grounds for this study. R. C. O., A. J. S., Y. G., S. S., D. G. V, D. F. L., and T. H. E. designed the study. R. C. O., A. J. S., A. L., and S. H. performed lignin content analysis experiments. R. C. O., A. J. S., Y. G., and S. S. analyzed the lignin content data. Y. G. performed reductive catalytic fractionation experiments, and Y. G. and S. S. analyzed the data. R. C. O., A. J. S., Y. G., D. F. L., and T. H. E. wrote and edited the initial manuscript drafts. R. C. O., A. J. S., A. L., S. H., and Y. O. contributed to the discussion of lignin content data. D. F. L., D. G. V., and T. H. E. acquired funding. All authors contributed to the overall discussion, reviewing, and final editing of the manuscript. The authors would like to thank Elvis O. Ebikade and Jeffrey L. Chang for their assistance in performing the initial RCF experiments and Kelly Walker for her assistance in making Fig. 2.

References

1 P. Gabrielli, L. Rosa, M. Gazzani, R. Meys, A. Bardow, M. Mazzotti and G. Sansavini, *One Earth*, 2023, **6**, 682–704.
2 H. Ritchie and P. Rosada, Energy mix, https://ourworldindata.org/energy-mix, (accessed 12/02/24).
3 Environmental Integrity Project, Oil & gas, https://environmentalintegrity.org/, (accessed 12/02/24).
4 U. Nations, Sustainable developments goals, https://sdgs.un.org/, (accessed 07/12/22).
5 C. O. Tuck, E. Pérez, I. T. Horváth, R. A. Sheldon and M. Poliakoff, *Science*, 2012, **337**, 695–699.
6 M. M. Abu-Omar, K. Barta, G. T. Beckham, J. S. Luterbacher, J. Ralph, R. Rinaldi, Y. Román-Leshkov, J. S. M. Samec, B. F. Sels and F. Wang, *Energy Environ. Sci.*, 2021, **14**, 262–292.
7 A. J. Ragauskas, G. T. Beckham, M. J. Biddy, R. Chandra, F. Chen, M. F. Davis, B. H. Davison, R. A. Dixon, P. Gilna, M. Keller, P. Langan, A. K. Naskar, J. N. Saddler, T. J. Tschaplinski, G. A. Tuskan and C. E. Wyman, *Science*, 2014, **344**, 1246843.
8 A. J. Shapiro, R. M. O'Dea, S. C. Li, J. C. Ajah, G. F. Bass and T. H. Epps III, *Annu. Rev. Chem. Biomol. Eng.*, 2023, **14**, 109–140.
9 S. Wang, L. Shuai, B. Saha, D. G. Vlachos and T. H. Epps III, *ACS Cent. Sci.*, 2018, **4**, 701–708.
10 L. Shuai, M. T. Amiri, Y. M. Questell-Santiago, F. Héroguel, Y. Li, H. Kim, R. Meilan, C. Chapple, J. Ralph and J. S. Luterbacher, *Science*, 2016, **354**, 329–333.
11 L. Shuai and B. Saha, *Green Chem.*, 2017, **19**, 3752–3758.
12 S. Wang, W.-X. Li, Y.-Q. Yang, X. Chen, J. Ma, C. Chen, L.-P. Xiao and R.-C. Sun, *ChemSusChem*, 2020, **13**, 4548–4556.
13 B. D. Titus, K. Brown, H.-S. Helmisaari, E. Vanguelova, I. Stupak, A. Evans, N. Clarke, C. Guidi, V. J. Bruckman, I. Varnagiryte-Kabasinskiene, K. Armolaitis, W. de Vries, K. Hirai, L. Kaarakka, K. Hogg and P. Reece, *Energy Sustain. Soc.*, 2021, **11**, 1–32.
14 M. Davis, L. Lambert, R. Jacobson, D. Rossi, C. Brandeis, J. Fried, B. English, R. Abt, K. Abt, P. Nepal, C. O'Dea and J. Prestemon, in *2023 Billion-Ton Report: An Assessment of U. S. Renewable Carbon Resources*, ed. M. H. Langholtz, Oak Ridge National Laboratory, Oak Ridge, TN, 2024. DOI: 10.23720/BT2023/2316170.
15 Y. Luo, R. M. O'Dea, Y. Gupta, J. Chang, S. Sadula, L. P. Soh, A. M. Robbins, D. F. Levia, D. G. Vlachos, T. H. Epps III and M. Ierapetritou, *Environ. Eng. Sci.*, 2022, **39**, 821–833.
16 T. Vangeel, D. M. Neiva, T. Quilhó, R. A. Costa, V. Sousa, B. F. Sels and H. Pereira, *Biomass Convers. Biorefin.*, 2021, **13**, 2029–2043.
17 Y. Liao, S.-F. Koelewijn, G. Van den Bossche, J. Van Aelst, S. Van den Bosch, T. Renders, K. Navare, T. Nicolaï, K. Van Aelst, M. Maesen, H. Matsushima, J. M. Thevelein, K. Van Acker, B. Lagrain, D. Verboekend and B. F. Sels, *Science*, 2020, **367**, 1385–1390.
18 B. Rietzler, M. Karlsson, I. Kwan, M. Lawoko and M. Ek, *Biomacromolecules*, 2022, **23**, 3349–3358.
19 A. W. Bartling, M. L. Stone, R. J. Hanes, A. Bhatt, Y. Zhang, M. J. Biddy, R. Davis, J. S. Kruger, N. E. Thornburg,

J. S. Luterbacher, R. Rinaldi, J. S. M. Samec, B. F. Sels, Y. Román-Leshkov and G. T. Beckham, *Energy Environ. Sci.*, 2021, **14**, 4147–4168.

20 R. Davis, L. Tao, E. C. D. Tan, M. J. Biddy, G. T. Beckham, C. Scarlata, J. Jacobson, K. Cafferty, J. Ross, J. Lukas, D. Knorr and P. Schoen, *Process design and economics for the conversion of lignocellulosic biomass to hydrocarbons: Dilute-acid and enzymatic deconstruction of biomass to sugars and biological conversion of sugars to hydrocarbons*, National Renewable Energy Lab. (NREL), Golden, CO (United States), United States, 2013.

21 A. Corona, M. J. Biddy, D. R. Vardon, M. Birkved, M. Z. Hauschild and G. T. Beckham, *Green Chem.*, 2018, **20**, 3857–3866.

22 S. Constant, H. L. J. Wienk, A. E. Frissen, P. Peinder, R. Boelens, D. S. van Es, R. J. H. Grisel, B. M. Weckhuysen, W. J. J. Huijgen, R. J. A. Gosselink and P. C. A. Bruijnincx, *Green Chem.*, 2016, **18**, 2651–2665.

23 M. Galbe and O. Wallberg, *Biotechnol. Biofuels*, 2019, **12**, 294.

24 R. M. O'Dea, P. A. Pranda, Y. Luo, A. Amitrano, E. O. Ebikade, E. R. Gottlieb, O. Ajao, M. Benali, D. G. Vlachos, M. Ierapetritou and T. H. Epps III, *Sci. Adv.*, 2022, **8**, eabj7523.

25 T. Renders, G. Van den Bossche, T. Vangeel, K. Van Aelst and B. Sels, *Curr. Opin. Biotechnol.*, 2019, **56**, 193–201.

26 V. Ponnuchamy, O. Gordobil, R. H. Diaz, A. Sandak and J. Sandak, *Int. J. Biol. Macromol.*, 2021, **168**, 792–805.

27 E. O. Ebikade, S. Sadula, Y. Gupta and D. G. Vlachos, *Green Chem.*, 2021, **23**, 2806–2833.

28 M. S. Kollman, X. Jiang, R. Sun, X. Zhang, W. Li, H.-m. Chang and H. Jameel, *Chem. Eng. J.*, 2023, **451**, 138464.

29 J. Ruwoldt, F. H. Blindheim and G. Chinga-Carrasco, *RSC Adv.*, 2023, **13**, 12529–12553.

30 S. J. H. M. Yusof, M. R. Zakaria, A. M. Roslan, A. A. M. Ali, Y. Shirai, H. Ariffin and M. A. Hassan, in *Lignocellulose for Future Bioeconomy*, ed. H. Ariffin, S. M. Sapuan and M. A. Hassan, Elsevier, 2019, pp. 265–285. DOI: 10.1016/B978-0-12-816354-2.00014-1.

31 N. L. Kapuge Dona, P. Y. Sauceda-Oloño and R. C. Smith, *J. Polym. Sci.*, 2025, **63**, 789–799.

32 I. Van Nieuwenhove, T. Renders, J. Lauwaert, T. De Roo, J. De Clercq and A. Verberckmoes, *ACS Sustainable Chem. Eng.*, 2020, **8**, 18789–18809.

33 P. Karagoz, S. Khiawjan, M. P. C. Marques, S. Santzouk, T. D. H. Bugg and G. J. Lye, *Biomass Convers. Biorefin.*, 2024, **14**, 26553–26574.

34 J. A. Emerson, N. T. Garabedian, D. L. Burris, E. M. Furst and T. H. Epps III, *ACS Sustainable Chem. Eng.*, 2018, **6**, 6856–6866.

35 A. L. Holmberg, K. H. Reno, N. A. Nguyen, R. P. Wool and T. H. Epps III, *ACS Macro Lett.*, 2016, **5**, 574–578.

36 A. L. Holmberg, N. A. Nguyen, M. G. Karavolias, K. H. Reno, R. P. Wool and T. H. Epps III, *Macromolecules*, 2016, **49**, 1286–1295.

37 J. B. Sluiter, R. O. Ruiz, C. J. Scarlata, A. D. Sluiter and D. W. Templeton, *J. Agric. Food Chem.*, 2010, **58**, 9043–9053.

38 Z. Jin, T. Akiyama, B. Y. Chung, Y. Matsumoto, K. Iiyama and S. Watanabe, *Phytochemistry*, 2003, **64**, 1023–1031.

39 T. Vangeel, T. Renders, K. Van Aelst, E. Cooreman, S. Van den Bosch, G. Van den Bossche, S. F. Koelewijn, C. M. Courtin and B. F. Sels, *Green Chem.*, 2019, **21**, 5841–5851.

40 A. Lourenço, J. Rencoret, C. Chemetova, J. Gominho, A. Gutiérrez, J. C. del Río and H. Pereira, *Front. Plant Sci.*, 2016, **7**, 1612.

41 J. Dou, H. Kim, Y. Li, D. Padmakshan, F. Yue, J. Ralph and T. Vuorinen, *J. Agric. Food Chem.*, 2018, **66**, 7294–7300.

42 W. Schutyser, T. Renders, S. Van den Bosch, S. F. Koelewijn, G. T. Beckham and B. F. Sels, *Chem. Soc. Rev.*, 2018, **47**, 852–908.

43 R. Evert, *Esau's Plant Anatomy: Meristems, Cells, and Tissues of the Plant Body-Their Structure, Function, and Development*, John Wiley & Sons, Inc, Publication, 2006.

44 C. Li, X. Zhao, A. Wang, G. W. Huber and T. Zhang, *Chem. Rev.*, 2015, **115**, 11559–11624.

45 G. F. Bass and T. H. Epps III, *Polym. Chem.*, 2021, **12**, 4130–4158.

46 T. Parsell, S. Yohe, J. Degenstein, T. Jarrell, I. Klein, E. Gencer, B. Hewetson, M. Hurt, J. Im Kim, H. Choudhari, B. Saha, R. Meilan, N. Mosier, F. Ribeiro, W. Nicholas Delgass, C. Chapple, H. I. Kenttämaa, R. Agrawal and M. M. Abu-Omar, *Green Chem.*, 2015, **17**, 1492–1499.

47 E. M. Anderson, M. L. Stone, R. Katahira, M. Reed, W. Muchero, K. J. Ramirez, G. T. Beckham and Y. Román-Leshkov, *Nat. Commun.*, 2019, **10**, 2033.

48 W. Boerjan, J. Ralph and M. Baucher, *Annu. Rev. Plant Biol.*, 2003, **54**, 519–546.

49 J. Ralph, C. Lapierre and W. Boerjan, *Curr. Opin. Biotechnol.*, 2019, **56**, 240–249.

50 T. Sariyildiz and J. M. Anderson, *For. Ecol. Manage.*, 2005, **210**, 303–319.

51 A. M. Taylor, B. L. Gartner and J. J. Morrell, *Wood Fiber Sci.*, 2002, **24**, 587–611.

52 O. A. Udume, G. O. Abu, H. O. Stanley, I. F. Vincent-Akpu and Y. Momoh, *Heliyon*, 2022, **8**, e10340.

53 K. Sahoo, R. Bergman and T. Runge, *Int. J. Life Cycle Assess.*, 2021, **26**, 1702–1720.

54 M. D. Berry and J. Sessions, *Appl. Eng. Agric.*, 2018, **34**, 109–124.

55 A. D. Richardson, T. F. Keenan, M. Migliavacca, Y. Ryu, O. Sonnentag and M. Toomey, *Agric. For. Meteorol.*, 2013, **169**, 156–173.

56 J. H. Jang, A. R. C. Morais, M. Browning, D. G. Brandner, J. K. Kenny, L. M. Stanley, R. M. Happs, A. S. Kovvali, J. I. Cutler, Y. Román-Leshkov, J. R. Bielenberg and G. T. Beckham, *Green Chem.*, 2023, **25**, 3660–3670.

57 J. K. Kenny, D. G. Brandner, S. R. Neefe, W. E. Michener, Y. Román-Leshkov, G. T. Beckham and J. W. Medlin, *React. Chem. Eng.*, 2022, **7**, 2527–2533.

58 Z. Liu, H. Li, X. Gao, X. Guo, S. Wang, Y. Fang and G. Song, *Nat. Commun.*, 2022, **13**, 4716.
59 G. G. Facas, D. G. Brandner, J. R. Bussard, Y. Román-Leshkov and G. T. Beckham, *ACS Sustainable Chem. Eng.*, 2023, **11**, 4517–4522.
60 D. G. Brandner, J. Gracia Vitoria, J. K. Kenny, J. R. Bussard, J. H. Jang, S. P. Woodworth, K. Vanbroekhoven, Y. Román-Leshkov and G. T. Beckham, *ACS Sustainable Chem. Eng.*, 2025, **13**, 12573–12582.
61 Y. Li, Y. Yu, Y. Lou, S. Zeng, Y. Sun, Y. Liu and H. Yu, *Angew. Chem., Int. Ed.*, 2023, **62**, e202307116.
62 J. Ralph, K. Lundquist, G. Brunow, F. Lu, H. Kim, P. F. Schatz, J. M. Marita, R. D. Hatfield, S. A. Ralph, J. H. Christensen and W. Boerjan, *Phytochem. Rev.*, 2004, **3**, 29–60.
63 L. Shuai, J. Sitison, S. Sadula, J. Ding, M. C. Thies and B. Saha, *ACS Catal.*, 2018, **8**, 6507–6512.